

# MRI morphological and volumetric study of the cingulate gyrus and its relevance in partial epileptic patients

Stéphane Kremer<sup>1, 2</sup>, Marc Braun<sup>2</sup>, Philippe Kahane<sup>1</sup>, F. Guillemin<sup>3</sup>, Jean-François Le Bas<sup>4</sup>, Alim Louis Benabid<sup>1</sup>

1. INSERM U318, Department of Neurosciences, University Hospital, Grenoble, France

2. Neuroradiology Department, University Hospital, Nancy, France

3. Clinical Epidemiology and Evaluation Department, Nancy, France

4. Neuroradiology Department, University Hospital, Grenoble, France

Received December 9, 2002 ; Accepted April 25, 2003

**ABSTRACT** – The cingulate gyrus (CG) is often involved during partial epileptic seizures.

The purpose of the study was to analyse the CG morphology and to measure the CG volume in epileptic patients, in order to detect subtle MRI abnormalities such as atrophy, which could be indicative of its implication in the epileptogenic area. The population consisted of 20 epileptic patients ( $31.2 \pm 9.4$  years) and 20 normal volunteers ( $31.8 \pm 7.7$  years). The epileptic patients underwent intracerebral recordings, and were sub-divided into five patients presenting with seizures involving the CG (CG 1), seven patients in whom the CG was only secondarily involved (CG 2) and eight patients in whom the CG was not involved at all (CG 3). All subjects were investigated by MRI (1.5 tesla Gyroscan Philips): axial T1w 3D Gradient Echo acquisitions, thickness 1.5 mm, reconstructions in all planes. At first, we described the sulcal limits of the CG, trying to define a “normalised CG”. In a second step, we segmented the CG intrasulcal grey matter using the “Surgiscope Scopeplan” (Elekta).

We compared (Mann and Whitney U test [ $\alpha=0.05$ ]), the CG volumes of CG 1 to CG 2 + 3, and the volume of CG 1 and of CG 1 + 2 + 3 to that of normal volunteers. There was no significant difference between CG 1 and CG 2 + 3 ( $P = 0.89$ ), between CG 1 and normal volunteers ( $P = 0.75$ ) or between CG 1 + 2 + 3 and normal volunteers ( $P = 0.83$ ). The volumetric analysis showed no atrophy of the CG in epileptic patients and did not distinguish the group in whom seizures involved the CG, from the other groups.

**KEY WORDS:** MR, central nervous system, epilepsy, cingulate gyrus

## Correspondence:

P. Kahane, M.D., Neurophysiopathologie de l'Épilepsie, Clinique Neurologique, CHU de Grenoble, BP217 X, 38043 Grenoble cedex, France.

Tel.: (33) 04 76 76 54 48

Fax: (33) 04 76 76 56 31

E-mail: philippe.kahane@ujf-grenoble.fr

For more than a decade, MRI has proved to be an essential examination in presurgical management of patients with medically intractable partial seizures [1]. In almost 90% of the cases, it shows space-occupying lesions or morphological abnormalities, which

can help to delineate the epileptogenic area [2]. In temporal lobe epilepsy, the most frequent form of drug resistant epilepsies (78% in the surgical series) [3], hippocampal sclerosis is present in 70% of the cases [3, 4], and seems to be a reliable marker of

the side, and even of the site of the epileptic discharges [1].

Since the cingulate gyrus is connected to several limbic structures through the Papez pathways [5-7], and since it can be involved in the propagation, or in the genesis of partial epileptic seizures [8, 9], it could be interesting to look for subtle MRI abnormalities in the cingulate gyrus, such as atrophy, which could be indicative of its implication in the epileptogenic area.

However, the cingulate gyrus is a complex anatomical structure, limited by several sulci or sulcus portions, with marked morphological variability, as shown by Ono *et al.* [10], explaining the difficulties in its delineation (*figure 1*).

The aims of this work were:

First to describe the sulcal limits of the cingulate gyrus, trying to define a "normalised cingulate gyrus".

Secondly, by using these limits, to look for cingulate gyrus atrophy, using volumetric MRI analysis, in patients with involvement of the cingulate gyrus in the epileptogenic area, as shown by stereotactic intracerebral EEG (SEEG).

## Patients and methods

### Patients

MRI examinations were performed for 20 patients (9 females and 11 males, age:  $31.2 \pm 9.39$  years), suffering from partial drug-resistant epilepsy, and for 20 healthy volunteers (10 females and 10 males, age:  $31.8 \pm 7.7$  years).

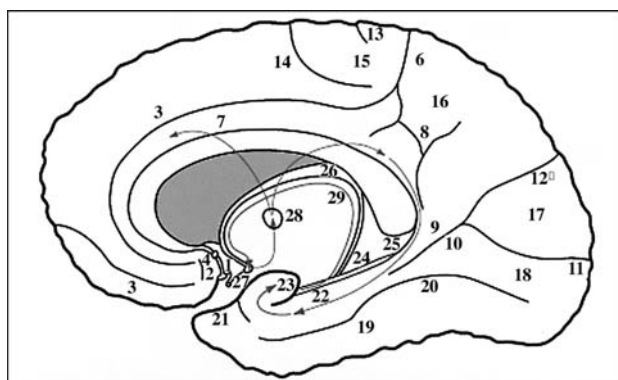


**Figure 1.** Sagittal and median view of the brain:

1: lamina terminalis; 2: anterior paraolfactory sulcus; 3: superior rostral sulcus; 4: subcallosal area; 5: cingulate sulcus; 6: marginal ramus of the cingulate sulcus; 7: cingulate gyrus; 8: subparietal sulcus; 9: isthmus of the cingulate gyrus; 10: antecaroline sulcus; 11: calcarine sulcus; 12: parieto-occipital sulcus; 13: central sulcus; 14: paracentral sulcus; 15: paracentral lobule; 16: precuneus (P1); 17: cuneus (O6); 18: O5; 19: T4; 20: collateral sulcus; 21: rhinal sulcus; 22: parahippocampal gyrus; 23: hippocampus head; 24: hippocampus body; 25: hippocampus tail; 26: fornix; 27: mamillary body; 28: anterior nucleus of the thalamus; 29: Papez pathways.

In the epileptic group, two were left-handed and 18 were right-handed, and in the volunteer group, 10 were left-handed and 10 were right-handed, as assessed by the Edinburgh inventory. In the epileptic group, the Wada-test confirmed a left hemispheric dominance for language in the 18 right-handed patients, and a right hemispheric dominance in the two left-handed patients.

Epileptic patients were included based upon the following criteria:

- adults more than 18 years old;
- negative history of psychiatric disorders;
- no obvious cerebral morphological lesion in the cingulate gyrus or in the neighboring structures on MRI;
- cingulate gyrus recording with at least one intracingulate electrode, during the intracerebral electrode recording procedure;
- planned and accepted surgical treatment of their epilepsy.

They were divided into three groups according to the involvement of the cingulate gyrus in the genesis of seizures, as defined by intracerebral recordings:

- CG 1 comprised five patients whose seizures clearly involved the cingulate gyrus, and which was therefore considered as part of the epileptogenic zone, thus justifying its resection (none of the resected specimens showed any 'specific' histological changes inside the CG)
- CG 2 comprised seven patients in whom the cingulate gyrus was only part of the discharges spread (no surgical resection).
- CG 3 comprised eight patients whose cingulate gyrus was not involved at all.

Informed consent was obtained from the volunteers, who were included in the study on the following criteria:

- adults more than 18 years old;
- negative history of neurologic and/or psychiatric disorders;
- no evident abnormality in the cingulate gyrus or surrounding structures on the MRI.

### Neuroimaging

All MR studies were performed at 1.5 T on a Gyroscan unit (Philips Medical Systems): axial T1w 3D Gradient Echo acquisitions, thickness: 1.5 mm, reformatting in all planes. The sulci (anterior paraolfactory sulcus, cingulate sulcus, and subparietal sulcus) were described on these MRI and the intrasulcal gray matter was segmented in a semi-automatic manner using the "Surgiscope Scopeplan" software by Elekta on a Hewlett-Packard workstation.

The limits were drawn manually in the frontal plane, cuts were apart and instant checking was available in the other planes simultaneously visualized. These measurements were performed on both cerebral hemispheres of the epileptic patients and normal volunteers.

The Scopeplan software starting from the presented limits, calculated the volume (cc) of the cingulate gyrus.

## Morphological study

The anterior limit of the cingulate gyrus is formed by the anterior paraolfactory sulcus and the lamina terminalis, the superior limit by the cingulate sulcus, then the subparietal sulcus and more posteriorly by the anterior part of the antecalcine sulcus, the inferior margin by the callosal sulcus, and the posterior border by the isthmus of the cingulate gyrus (*figure 1*). We studied the major sulci that showed, in agreement with Ono's description [10], important morphological variations, namely the cingulate sulcus, the subparietal sulcus and the anterior paraolfactory sulcus.

For the cingulate sulcus the following features were noted:

- the position of its anterior end, according to Ono's classification [10] (*figure 2*);
- its connection with the superior rostral sulcus;
- the presence of interruptions, defined as a rupture of the continuity of the sulcus, visible on all MRI planes (*figure 3*);
- double parallel patterns, defined as a division of the cingulate sulcus in 2 parallel subsulci, not connected with each other (*figure 3*);
- The presence of an intracingulate sulcus, defined as a sulcus starting at the anterior part of the corpus callosum and joining the middle part of the cingulate sulcus (*figure 3*);

For the subparietal sulcus (*figure 4*): according to Ono's classification [10], it was postulated that the subparietal sulcus has, most of the time, an H-pattern, defined by a horizontal sulcus prolonging posteriorly the cingulate sulcus, and two upwardly-oriented side-branches, and two downwardly-oriented side-branches. The following features were noted:

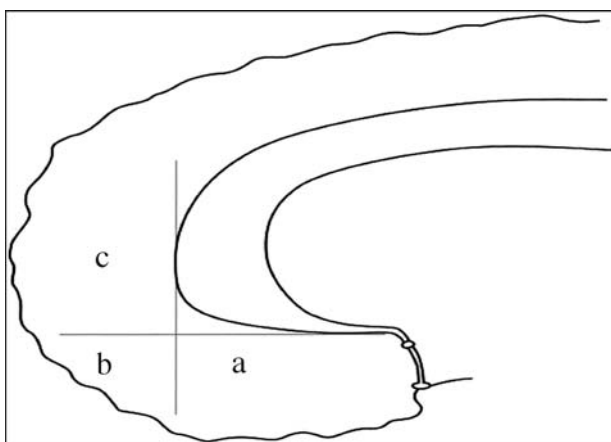


**Figure 2.** Position of the anterior end of the cingulate sulcus (Ono): **a**: sub-callosal; **b**: supra-orbital; **c**: prefrontal.

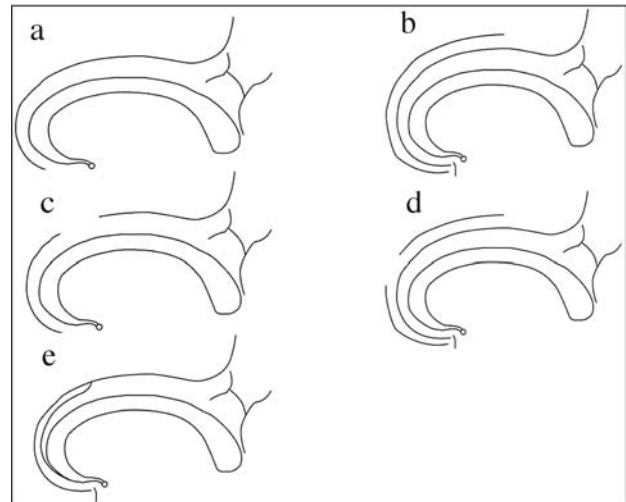


**Figure 3.** Examples of anatomical variations of the cingulate sulcus: **a**: single cingulate sulcus; **b**: double parallel pattern; **c**: single cingulate sulcus with one interruption; **d**: double parallel pattern with one interruption of the external sulcus; **e**: intracingulate sulcus.

- the number of side branches;
- the connection with the posterior end of the cingulate sulcus and the route of connection;
- double parallel patterns;
- atypical patterns.

For the anterior paraolfactory sulcus, the following features were studied:

- whether or not it was distinguishable;
- the connection of the anterior paraolfactory sulcus with the cingulate sulcus.

These analyses were performed blind on both cerebral hemispheres of each patient, by two independent observers (SK, MB).

Statistical analysis was performed using the Chi square test or Fisher exact test, a *P* value of 0.05 was regarded as

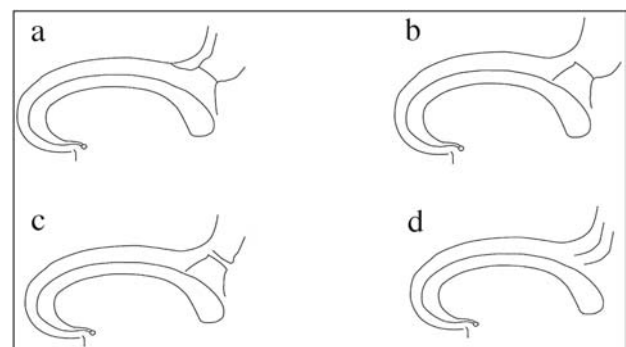


**Figure 4.** Examples of anatomical variations of the subparietal sulcus:

- a**: H pattern, connected through the antero-inferior side-branch with the cingulate sulcus; **b**: subparietal sulcus with single upwardly directed side-branch, not connected with the cingulate sulcus; **c**: double parallel pattern; **d**: atypical pattern.

significant. Due to the small number of patients in subgroups, the different subgroups were compared as follows: epileptic hemispheres of CG 1 (patients who presented seizures which involved the cingulate gyrus) with those of CG 2 + 3 (patients in whom the cingulate gyrus was only part of the discharges spreading or was not involved at all), CG 1 with volunteers, CG 1 + 2 + 3 with volunteers, for the presence of the different anatomical variations.

Inter-rater reliability was evaluated by the kappa index.

## Volumetric analysis

The cingulate gyrus was measured after segmentation of the cortical grey matter, following the different sulci as anatomical limits defined above.

These analyses (figure 5) were performed blind on both cerebral hemispheres of each patient, by two independent observers (SK, MB), each one unaware of the results of the other observer.

Statistical analysis was performed using the Mann and Whitney U-test. The average volume of the cingulate gyrus was compared in the different subgroups (epileptic hemispheres of CG 1 (patients who presented seizures which involved the cingulate gyrus), with CG 2 + 3 (patients in whom the cingulate gyrus was only part of the discharges spreading or was not involved at all), CG 1 with volunteers, CG 1 + 2 + 3 with volunteers).



**Figure 5.** Delimitation of the cingulate gyrus in the coronal plane (Scopeplan of Elekta's Surgiscope): Upper left corner shows the final extracted volume. The other corners show the limits in axial (upper right), sagittal (down left) and coronal planes (down right). The coronal plane was the most useful to delineate the margins, the sagittal one was used to check the limits, especially the posterior portions (isthmus) and the anterior one (anterior paraolfactory sulcus).

## Results

### Morphological study

#### 1) Inter-rater reliability

The inter-rater reliability was excellent, with a kappa index superior to 0.9 in all cases.

#### 2) Statistical analysis

There was no significant statistical difference between the different subgroups, with the exception of the double parallel pattern that showed significantly more interruptions of the external portion in the volunteer group, than in the group CG 1 + 2 + 3 ( $P = 0.019$ , Chi square test). Nevertheless, these results allowed us to pool the 80 hemispheres, for the description of the sulcal variability.

#### 3) Description of the sulcal variations (table 1-3) (figure 6 and 7)

### Volumetric study

#### 1) Inter-rater reliability

The inter-rater reliability was excellent, with a intraclass correlation coefficient  $\rho = 0.92$  in the volunteer group and  $\rho = 0.93$  in the epileptic group.

#### 2) Statistical analysis

No statistically significant difference was found between the mean volume in CG 1 ( $12.58 \pm 2.84$ ) and CG 2 + 3 ( $12.56 \pm 2.57$ ) ( $P = 0.89$ ), between the mean volume in CG 1 and the volunteer group ( $12.56 \pm 2.56$ ) ( $P = 0.75$ ), or between the mean volume in CG 1 + 2 + 3 ( $12.46 \pm 1.94$ ) and the volunteer group ( $P = 0.83$ ).

**Table 1. Cingulate sulcus: morphological description.**

Cingulate sulcus	N	%
Position anterior end: a	68	85
Position anterior end: b	9	11
Position anterior end: c	3	4
Double parallel pattern	33	41
Single sulcus pattern	47	59
No interruption (single sulcus pattern)	29	62
One interruption	14	30
Two interruptions	4	8
No interruption internal sulcus (double parallel pattern)	31	94
One interruption	2	6
No interruption external sulcus (double parallel pattern)	19	58
One interruption	14	42
Intracingle sulcus	16	20
Cingulate sulcus-superior rostral sulcus connection	8	10

**Table 2. Subparietal sulcus: morphological description.**

Subparietal sulcus	N	%
Cingulate sulcus-subparietal sulcus connection	48	60
Route of connection antero-inferior sidebranch (Ant <)-marginal ramus (MR)	21	44
Ant > -MR	23	48
Horizontal branch of the H-MR	4	8
Double parallel pattern	3	4
Single sulcus	72	90
Atypical	5	6
Upwardly oriented sidebranches 1	11	14
Two	57	71
Three	7	9
Atypical	5	6
Downwardly oriented sidebranches 1	7	9
Two	62	77
Three	6	8
Atypical	5	6
H pattern	46	57

**Table 3. Anterior paraolfactory sulcus: morphological description.**

Anterior paraolfactory sulcus	N	%
Anterior paraolfactory sulcus distinguishable	56	70
Anterior paraolfactory sulcus not distinguishable	24	30
Connection anterior paraolfactory sulcus-cingulate sulcus	34	61

The volumetry of the cingulate gyrus does not distinguish the different subgroups from each other.

## Discussion

### Description of the sulcal variability

In the double-parallel pattern of the cingulate sulcus, there were significantly more interruptions of the external portion in the volunteer group, than in the group CG 1 + 2 + 3 ( $P = 0.019$ , Chi square test), but there is no pathophysi-

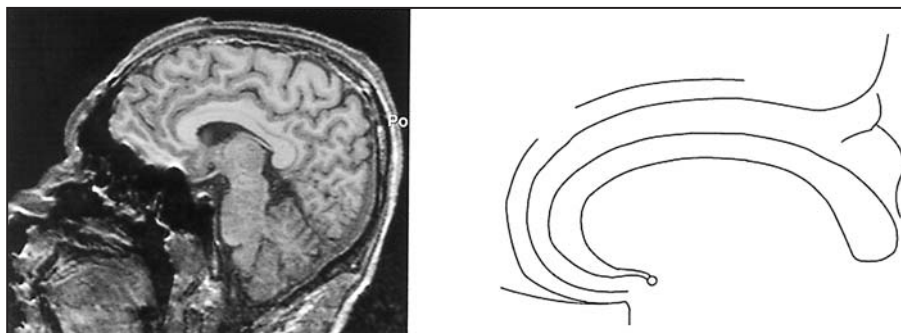


**Figure 6.** Sagittal median MRI of the brain: example 1: Double parallel cingulate sulcus, connected with the superior rostral sulcus, one interruption of the external sulcus. Subparietal sulcus with two downwardly and one upwardly directed side-branches, not connected with the cingulate sulcus. Anterior paraolfactory sulcus distinguishable, not connected with the cingulate sulcus.

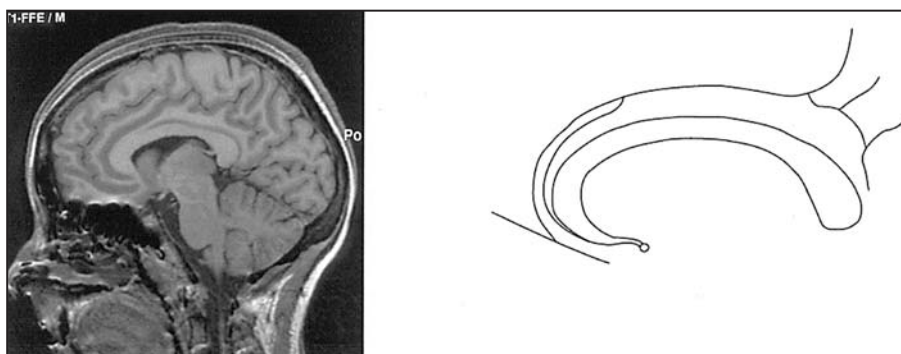


**Figure 7.** Sagittal median MRI of the brain: example 2: Single cingulate sulcus with an intracingulate sulcus. Anterior end in b position, connection with the superior rostral sulcus. H pattern of the subparietal sulcus, connected with the cingulate sulcus.



ological explanation for this result. No anatomical reason may explain such a difference.

The description of the sulcal variability was similar to that of other authors [10-12]. The few differences are related to a different definition of the sulci or to methodological differences.

The main differences in definition concerned the double parallel patterns of the cingulate sulcus described by Ono [10]. Actually, Paus [12] considers the external sulcus as the paracingulate sulcus and describes it as present in 85% of right-handed cases and in 92% of left-handed cases. But in 48% of the right-handed cases and 38% of the left-handed cases it consisted of only a few vertical branches [12], a pattern that has been excluded from the current study, considering only the horizontal sulci parallel to the cingulate sulcus, referred to as the prominent paracingulate sulcus by Paus [12]. The vertical branches belong to other frontal lobe structures and not to the cingulate gyrus *per se*.

The intracingulate sulcus, present in 20% of the cases in the current study, corresponds to Paus, intralimbic sulcus, and is found in 6% on the right side and in 4% on the left side [11, 12]. This difference could be explained by the recruitment difference between the two studies, as Paus's study pooled 247 subjects. Moreover this sulcus is not described by Ono [10].

Other differences may be explained by the properties of the MRI. Actually, more connections were found between the cingulate sulcus and the subparietal sulcus than by Ono [10] (table 5, Ono – 36% on the right side and 28% on the left side). MRI displays very thin slices (1.5 mm), and simultaneous multiplanar views allowing study of the depth of the sulci, detecting connections under the brain surface.

However, MRI is not suitable for a study of very superficial sulci, as they disappear within the slice thickness. This is, for example, the case for the anterior paraolfactory sulcus, described by Ono in 92% of the cases on the right side and in 72% on the left side, but in 20% on the right side and in 16% on the left side in the current series, it is represented by a smooth depression, not visible on MRI [10].

Another difference between this study and previous studies [10-12], is that the sulcal variability in the right hemispheres has not been compared to the left hemispheres. Paus has described significant differences between the two hemispheres in the cingulate sulcus [11-12].

However, in most of the studies, only right handed subjects were included. The series of subjects in this study was constituted by right and left handed subjects, and the cerebral dominance for language was assessed by an Amobarbital test, which can be considered as the gold standard, only in the epileptic group. Cerebral dominance was assessed only by Edinburgh test in the volunteer group.

## Methodological aspect

The cingulate gyrus is a complex anatomical structure. It presents great sulcal variability, and in some portions no sulcal limit is found, for example at the isthmus of the cingulate gyrus, or in the case of an interruption in a sulcus or between two sulci. The definition of a "normalised cingulate gyrus", based only on sulcal limits is not possible, and it is necessary to define arbitrary limits, based on previous studies [13-15].

There were difficulties also in the double parallel pattern of the cingulate sulcus in defining the cingulate gyrus limits. Whether the area 32 of Brodmann, situated between the two branches of the cingulate sulcus, belongs to the cingulate cortex remains a questionable issue. Pandya, Room and Albanese [13, 16, 17] consider, on studies based on the area 32 connections, that it does not belong to the anterior cingulate gyrus cortex, but to the prefrontal cortex. Talairach and Vogt [15, 18, 19] consider, based on of cytoarchitectonic studies, that it represents a transitional fronto-limbic cortex, though belonging to the cingulate gyrus. This study is in agreement with these last authors, and we consider the external branch of the cingulate sulcus as the superior limit of the cingulate gyrus.

Moreover, the marginal ramus and the secondary, upwardly vertical branches of the cingulate sulcus and of the subparietal sulcus were excluded from the delimitation of the cingulate gyrus. Actually, the marginal ramus penetrates the parietal lobe and does not contain cingulate cortex. The same reasons apply to the secondary branches, penetrating the parietal lobe or the frontal lobe. The last limitation to this study, was the number of patients showing implication of the cingulate gyrus in the genesis of the epileptic seizures. Only 5 patients justifying the resection of the cingulate gyrus, were included in the study, and it is statistically difficult to show small losses of volume in the cingulate gyrus.

## Volumetry of the cingulate gyrus in the epileptic patient

There was no difference in cingulate gyrus volume between the different subgroups of patients and the healthy volunteers. The volumetry of the cingulate gyrus did not allow us to distinguish the group in whom the cingulate gyrus is involved in the genesis of the seizures, from the other groups. There was no atrophy of the cingulate gyrus in the epileptic group, unlike the hippocampal sclerosis, which is found in 72% of the epilepsies involving the temporal lobe [3].

Different hypotheses have been proposed to explain the appearance of hippocampal sclerosis, but the most frequently cited is a past history of convulsions, which could have been due to fever or to a temporal malformative lesion [3, 4, 20].

Moreover, it has been demonstrated that epileptic seizures induced by kindling, produced hippocampal lesions, and

that hippocampal neurons are particularly vulnerable to repeated seizures, compared to other neuronal populations, which, when submitted to the same treatment did not demonstrate any degeneration [20, 21]. This leads to the hypothesis that cingulate neurons are less vulnerable to repeated seizures than the hippocampic neurons. The fact that repeated seizures induce atrophy seems to be a specific property of hippocampal neurons, and of structures directly connected to the hippocampus, such as the fornix, the mamillary bodies and the entorhinal cortex [1, 22-26]. □

## References

1. Duncan JS. Imaging and epilepsy. *Brain* 1997; 120: 339-77.
2. Jackson GD. New techniques in magnetic resonance imaging and epilepsy. *Epilepsia* 1994; 35: 2-13.
3. Pasquier B, Peoc'h M, Barnoud R, et al. Predilection lésionnelle pour le lobe temporal dans l'épilepsie partielle pharmacorésistante: aspect neuropathologique d'une série de 180 patients. *Boll Lega It Epil* 1996; 95: 57-64.
4. Jackson GD, Berkovic SF, Tress BM, et al. Hippocampal sclerosis can be reliably detected by magnetic resonance imaging. *Neurology* 1990; 40: 1869-75.
5. Papez J. A proposed mechanism of emotion. *Arch Neurol Psychiatry* 1937; 38: 725-43.
6. Duvernoy HM. The human hippocampus. 2<sup>nd</sup> edition. Berlin: Springer Verlag, 1998; 213.
7. Mark LP, Daniels DL, Naidich TP, Hendrix LE. Limbic connections. *AJNR* 1995; 16: 1303-6.
8. Bancaud J, Talairach J, Geier S, et al. Manifestations comportementales induites par la stimulation électrique du Gyrus Cingulaire antérieur chez l'homme. *Rev Neurol* 1976; 132: 705-24.
9. Bancaud J, Talairach J. Clinical semiology of frontal lobe seizures. *Adv Neurol* 1992; 57: 3-58.
10. Ono M, Kubik S, Abernathy CD. *Atlas of the cerebral sulci*. Stuttgart: Thieme, 1990: 217.
11. Paus T, Otaky N, Caramanos Z, et al. *In vivo* morphometry of the intrasulcal gray matter in the human cingulate, paracingulate, and superior rostral sulci: hemispheric asymmetries, gender differences and probability maps. *J Comp Neurol* 1996; 376: 664-73.
12. Paus T, Tomaiuolo F, Otaky N, et al. Human cingulate and paracingulate sulci: pattern, variability, asymmetry, and probabilistic map. *Cereb Cortex* 1996; 6: 207-14.
13. Albanese AM, Merlo AB, Mascitti TA, et al. Inversion of the hemispheric laterality of the anterior cingulate gyrus in schizophrenics. *Biol Psychiatry* 1995; 38: 13-21.
14. Hutsler JJ, Loftus WC, Gazzaniga MS. Individual variation of cortical surface area asymmetries. *Cereb Cortex* 1998; 8: 11-7.
15. Vogt BA, Nimchinsky EA, Vogt LJ, Hof PR. Human cingulate cortex: surface features, flat maps, and cytoarchitecture. *J Comp Neurol* 1995; 359: 490-506.
16. Pandya DN, Van Hoesen GW, Mesulam MM. Efferent connections of the cingulate gyrus in the rhesus monkey. *Exp Brain Res* 1981; 42: 319-30.
17. Room P, Russchen FT, Groenewegen HJ, Lohman AH. Efferent connections of the prelimbic (area 32) and the infra-limbic (area 25) cortices: an anterograde tracing study in the cat. *J Comp Neurol* 1985; 242: 40-55.
18. Talairach J, Szikla G, Tournoux P, Prosalenti A, Bordas-Ferrier M. *Atlas d'anatomie stéréotaxique du télencéphale*. Paris: Masson, 1967: 303.
19. Talairach J, Tournoux P. *Co-planar stereotaxic atlas of the human brain. 3-dimensional proportional system: an approach to cerebral imaging*. Stuttgart: Thieme, 1988: 122.
20. Cavazos JE, Das I, Sutula TP. Neuronal loss induced in limbic pathways by kindling: evidence for introduction of hippocampal sclerosis by repeated brief seizures. *J Neurosci* 1994; 14: 3106-21.
21. Moshe SL. Brain injury with prolonged seizures in children and adults. *J Child Neurol* 1998; 13: 30-2.
22. Chan S, Erickson JK, Yoon SS. Limbic system abnormalities associated with mesial temporal sclerosis: a model of chronic cerebral changes due to seizures. *Radiographics* 1997; 17: 1095-110.
23. Baldwin GN, Tsuruda JS, Maravilla KR, et al. The fornix in patients with seizures caused by unilateral hippocampal sclerosis: detection of unilateral volume loss on MR images. *AJR* 1994; 162: 1185-9.
24. Lau TN, Lui FKH, Chua GE, et al. MRI of the fornix and mamillary body in temporal lobe epilepsy. *Neuroradiology* 1997; 39: 551-5.
25. Yamada K, Shrier DA, Rubio A, et al. MR imaging of the mamillothalamic tract. *Radiology* 1998; 207: 593-8.
26. Mamourian AC, Brown DB. Asymmetric mamillary bodies: MR identification. *AJNR* 1993; 14: 1332-5.